

Header Recognition Utilizing an All-Optical Reservoir with Delay-Bandwidth-Product-Maximized Double-Ring Resonators

Zheng Li¹, Zongze Li², Xiaoyan Zhou¹, Guanju Peng¹, Yuhao Guo³, Wenwei Xu^{3,*}, and Lin Zhang^{1,2,*}

¹Tianjin Key Laboratory of Integrated Opto-electronics Technologies and Devices, School of Precision Instruments and Engineering, Tianjin University, Tianjin 300072, China. Email: *xuwenwei@huawei.com, *lin_zhang@tju.edu.cn

²Peng Cheng Laboratory, Shenzhen 518038, China

³Huawei Technologies Co., Ltd, Shenzhen 518129, China

Abstract: The delay-bandwidth product in double-ring resonators (DRRs) is optimized using reinforcement learning. Then, the optimized DRRs are used to build an all-optical reservoir for optical packet header recognition, enabling a word-error rate as low as 9×10^{-4} . © 2023 The Author(s)

1. Introduction

Recently, integrated microring resonators (MRRs) have become key structures for achieving versatile functional devices in a small area [1,2], not only employed in sensors but also useful in optical communication systems [3-5]. The recognition of optical packet header is one of the significant functions of optical networks [6]. The current techniques for packet header recognition mainly utilize several optoelectronic devices, such as fiber-optic delay lines and vertical-cavity surface-emitting lasers, which are difficult to integrate on a chip [7,8]. Therefore, a photonic reservoir consisting of MRRs is a great opportunity for optical packet header recognition, in which the implementations of broadband MRRs with large and controllable group delay, i.e., a large delay-bandwidth product (DBP), play a key role.

Conventionally, heuristic or genetic algorithms have been used to optimize the DBP of a single resonator [9], although these suffer from heavy computation loads or inevitable convergence errors [10]. In contrast, AI-based methods with fast convergence time and low convergence error have recently emerged as a promising approach for resource allocation in optical networks [11], color generation in dielectric nanostructures [12], and optical multi-layer thin film design [12] and so on. However, how to efficiently optimize double-ring resonators (DRRs) to achieve the maximum DBP still remains unexplored. In particular, it would be of great interest to utilize such AI-enabled photonic devices to build an advanced on-chip optical reservoir for higher-level system applications, e.g., header recognition in optical networks.

Here, we maximize the DBP of four types of DRRs using reinforcement learning, known as asynchronous advantage actor-critic (A3C) algorithm. Intriguingly, we note that the DBPs of the cascaded ring, parallel ring, and embedded ring reach the same maximum, but the DBP of the 3×3 coupler ring is about half of the formers, which deepens our understanding of the double-ring resonators. An all-optical reservoir is built with the optimized DRRs for optical packet header recognition, enabling a greatly reduced word-error rate (WER) by two orders of magnitude to as low as 9×10^{-4} and significantly shrunk chip size.

2. Reservoir configuration, group delay unit optimization and results

We form an all-optical reservoir with DRRs as the nodes for optical packet header recognition, as shown in Fig. 1(a). The header signals are processed by mask and transmitted by the reservoir, which can be trained via ridge regression to realize the optical header recognition task. The bit rate and the bandwidth are set to 10 Gbps, and 50 GHz, respectively.

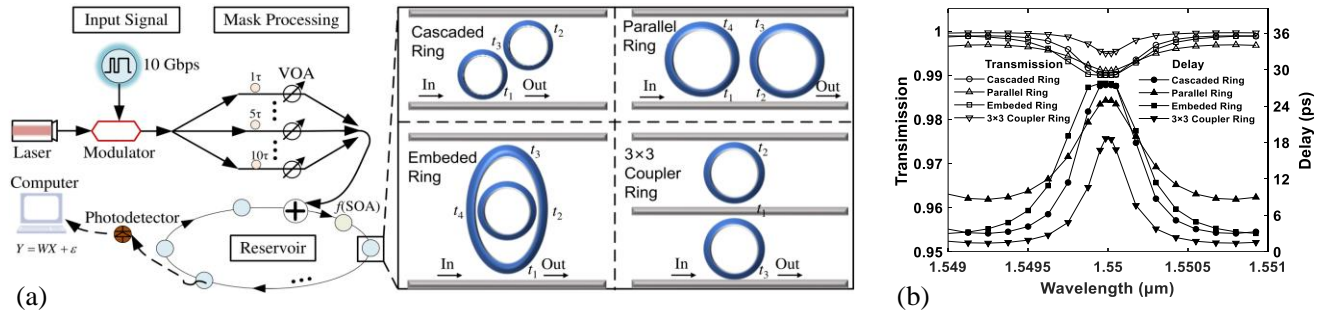


Fig. 1 (a) An all-optical reservoir consists of a nonlinear activation unit based on a semiconductor optical amplifier (SOA), a photodetector, and optical delay nodes, which are considered to be one of the four types of DRRs. (b) The transfer function in power and group delay for the four types of DRRs vs. wavelengths with the parameter combinations optimized using AI algorithm. The maximum DBPs of the cascaded ring resonators, parallel ring resonators, and embedded ring resonators reach the same value, which is 1395 ps·GHz and it is about twice of that of the 3×3 coupler ring resonators.

The DRRs are comprised of lithium niobate waveguides, and the waveguide loss is set to 0.1 dB/cm. We set radii of the DRRs to be $R = 70 \mu\text{m}$ and the waveguide cross-section to be $3 \mu\text{m} \times 150 \text{ nm}$ (width \times height), resulting in an effective refractive index of 1.9 at a resonant wavelength of $1.55 \mu\text{m}$. The variables to be optimized in DRRs are coupling coefficients.

As a representative, we show that different algorithms are used to maximize the DBP of the cascaded ring resonators, as shown in Fig. 2(b). The results show that the DBP reaches the maximum of 1395 ps·GHz with a 27.0 ps delay and 51.7 GHz bandwidth, which is superior to the state-of-the-art performance. The optimized coupling coefficients are $t_1 = 0.902$, $t_2 = 0.011$, and $t_3 = 0.354$. We note that the optimized DBP of the cascaded ring resonators has a good performance on the "flat-top" delay profiles at the resonant wavelength.

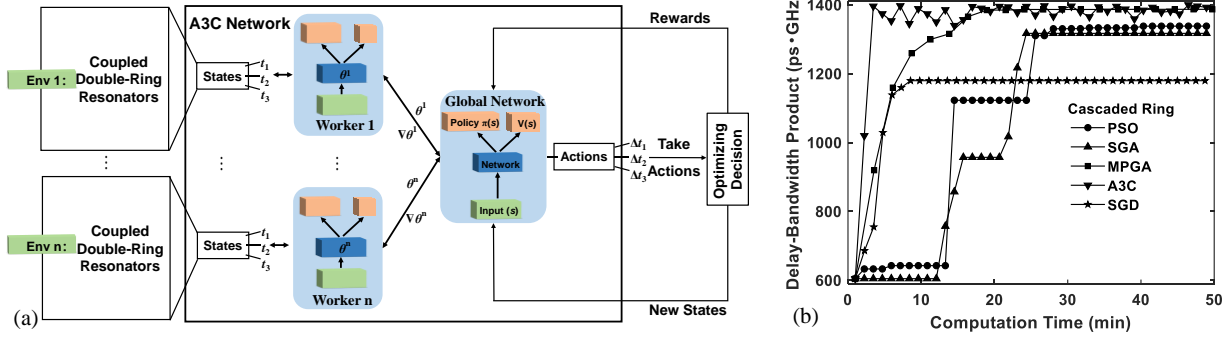


Fig. 2 (a) Our A3C reinforcement learning algorithm. n -DRRs, serving as the optimization environments, interact with the A3C network. The rewards, states, and actions of the A3C network are DBP, coupling coefficients, and changes of coupling coefficients, respectively. The global network and workers in the A3C network have the same architecture and parameters. (b) For the cascaded DRRs as an example, the DBP over computation time taken by different algorithms. The inference time of the A3C algorithm is less than 5 minutes. The inference time and convergence error of the A3C algorithm are significantly better than the traditional algorithms, including particle swarm optimization algorithm (PSO), simple genetic algorithm (SGA), multi-population genetic algorithm (MPGA), and stochastic gradient descent algorithm (SGD).

Finally, for a fair comparison, in the case of different node delays (τ_{delay}) and number of nodes (N) in the reservoir, we constrain the total delay of a loop $\theta = N \times \tau_{\text{delay}}$ to be the same, which is 500 ps, as shown in Fig. 3(a). Here, we show the results that the cascaded ring resonator is the node of the reservoir. When $T = 3 \text{ ns}$ and $\tau_{\text{delay}} = 25 \text{ ps}$, the WERs achieve 5×10^{-4} and 9×10^{-4} for the 3-bit and 6-bit header signals, respectively, which are two orders of magnitude better than the previously reported results [13,14].

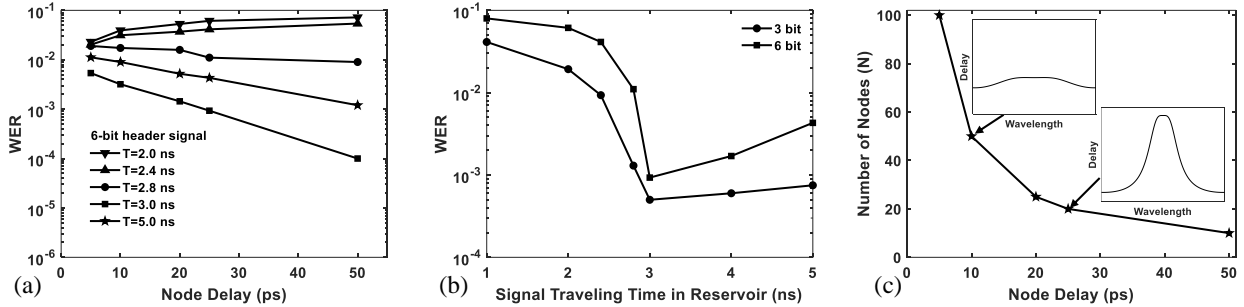


Fig. 3. (a) The word error rate (WER) in header recognition of 6-bit optical packet header signals. The traveling time of the header signal in the reservoir (T) is the multiple times of the node delay (τ_{delay}). When $T < 2.5 \text{ ns}$, due to the small number of samples, the WER increases with τ_{delay} . When $T > 2.5 \text{ ns}$, the WER decreases with τ_{delay} . (b) At $\tau_{\text{delay}} = 25 \text{ ps}$, the WERs of 3-bit and 6-bit header signals with T . Due to the optical loss of the node, the WERs of 3-bit and 6-bit header signals first decrease and then slightly increase with T . At $T = 3 \text{ ns}$, the WERs of 3-bit and 6-bit header signals reach the minima, i.e., 5×10^{-4} and 9×10^{-4} , respectively, two orders better than the previous results [13,14]. (c) The required number of nodes (N) vs. τ_{delay} of each node. The delay spectra for $\tau_{\text{delay}} = 10$ and 25 ps are in the inset.

Our work reveals that, although placed in different configurations, various DRRs reach the same maximum DBP, pointing to a global upper limit for any other possible DRR structures. Due to the key role of ring resonator devices in integrated photonics, exploring their full parameter space via AI algorithms would pave the way to miscellaneous application scenarios, in which one may aim at the steepness of device transfer functions, resonance-enhanced in-cavity power, to name a few.

3. References

- [1] Q. Li et al., OE **18**, 8367-8382, 2010.
- [2] L. McKenzie-Sell et al., PRB **99**, 140414, 2019.
- [3] J.-X. Cai et al., JLT **36**, 114-121, 2017.
- [4] C. Ranaweera et al., IEEE Network **26**, 22-27, 2012.
- [5] F. Karinou et al., PTL **27**, 1872-1875, 2015.
- [6] M. S. Rasras et al., PTL **20**, 694-696, 2008.
- [7] T. Tsurugaya et al., CLEO, 1-2, 2021.
- [8] I. Kang et al., ECOC, 1-2, 2008.
- [9] P. Chamorro-Posada et al., JLT **32**, 1477-1481, 2014.
- [10] A. Jiang et al., SCI REP-UK **10**, 12780, 2020.
- [11] D. Rafique et al., J Opt Commun Netw **10**, 126-143, 2018.
- [12] I. Sajedian et al., OE **27**, 5874-5883, 2018.
- [13] T. Katayama et al., PTL **25**, 802-805, 2013.
- [14] H. Zhao et al., Optik **157**, 951-956, 2018.